Royal Netherlands Institute for Sea Research

[Article begins on next page]

Carrying capacity of *Saccharina latissima* cultivation in a Dutch coastal bay: a modeling assessment

Long Jiang[1,2,3*], Lander Blommaert[3], Henrice M. Jansen[4,5], Ole Jacob Broch[6], Klaas R. Timmermans[3], and Karline Soetaert[3]

[1]Key Laboratory of Marine Hazards Forecasting, Ministry of Natural Resources, Hohai University, Nanjing, 210098, China

[2]Key Laboratory of Ministry of Education for Coastal Disaster and Protection, Hohai University, Nanjing, 210098, China

[3]NIOZ Royal Netherlands Institute for Sea Research, Department of Estuarine and Delta Systems, P.O. Box 140, 4400 AC Yerseke, the Netherlands

[4]Wageningen Marine Research, Wageningen University & Research, P.O. Box 77, 4400, AB, Yerseke, the Netherlands

[5]Aquaculture and Fisheries group, Department of Animal Sciences, Wageningen University & Research, PO Box 338, 6700 AH Wageningen, The Netherlands

[6]SINTEF Ocean, Environment and New Resources, 7465 Trondheim, Norway

*Corresponding author: tel: +86 83786641; e-mail: ljiang@hhu.edu.cn.

Abstract

Kelp cultivation receives increasing interest for its high-value products and ecological services, especially in Europe and North America. Before industrial kelp farming in marine ecosystems continue to scale up, evaluation of the site-wide production relative to ecological carrying capacity of the identified system is essential. For this purpose, a mechanistic kelp model was developed and applied for hypothetical numerical experiments of expanding the farming area in a Dutch coastal bay (the Eastern Scheldt), where cultivation of *Saccharina latissima* (sugar kelp) is emerging. The kelp model was implemented within a three-dimensional hydrodynamic-biogeochemical model to account for the environmental interactions. The model captured the seasonal growth dynamics of *S. latissima*, as well as its carbon and nitrogen contents measured at the Eastern Scheldt pilot sites. The model results suggest that expanding the kelp farming area to ~1%–30% of the bay (representing ~3.4–75 kt harvest dry weight in the 350-km^2 bay) had the potential to weaken the spring bloom and thereby affected the coexisting shellfish culture in the bay. Competition between *S. latissima* and phytoplankton mostly occurred in late spring for nutrients (dissolved inorganic nitrogen). The ecological carrying capacity should be weighed according to these negative impacts. However, the production carrying capacity was not reached even when farming ~30% of the Eastern Scheldt, i.e., harvesting totally 75 kt dry mass, given that the simulated overall *S. latissima* production kept increasing with the farming activity. Our modeling approach can be applied to other systems for *S. latissima* cultivation and assist in assessing carrying

45 capacity and environmental impacts.

46 **Keywords:** the Eastern Scheldt, seaweed farming, three-dimensional mechanistic

47 model, carrying capacity, phytoplankton

48 **Introduction**

49 Seaweed farming is gaining increasing interest globally, for its economic and

50 ecological values (Hasselström et al., 2018; Boderskov et al., 2021), and the world

51 seaweed production has tripled since the early 2000s (FAO, 2020). The cultivated

52 seaweed provides sustainable sources for food, feed, biofuels, pharmaceuticals,

53 cosmetics, and other biotechnological products at no cost of agricultural land,

54 freshwater irrigation, fertilizers, and pesticides needed by terrestrial crops (Forbord et

55 al., 2012). Meanwhile, the cultured seaweed is able to assimilate excessive nutrients

56 from river runoff and fish farms, mitigating coastal eutrophication and hypoxia, to

57 provide feeding ground, shelter, and nursery habitats for local organisms, increasing

58 biodiversity, and to damp onshore waves, preventing shoreline erosion (Sanderson et

59 al., 2012; Broch et al., 2013; Handå et al., 2013; Nielsen et al., 2014; Xiao et al.,

60 2017; Hasselström et al., 2018). In addition to these local ecosystem services, the

61 macroalgae cultivation, if increased to a considerable scale, may sequester a

62 substantial amount of carbon to mitigate climate change (Duarte et al., 2017; Krause-

63 Jensen et al., 2018; Froehlich et al., 2019). On top of the positive ecosystem services,

64 negative environmental effects of seaweed aquaculture include altering water flow

65 (Campbell et al., 2019) and polluting the seawater when fertilized (Ogawa and Fujita,

66 1997), whereas negative impacts seem to be limited if applied at suitable scales in

67   some other systems (Walls et al., 2017; van der Molen et al., 2018).

68   Sugar kelp (*Saccharina latissima*), a large brown alga naturally distributed in

69   temperate and polar seas (Bartsch et al., 2008), is one of the most commonly

70   cultivated macroalgal species in North America and Europe (Lubsch and

71   Timmermans, 2019; Venolia et al., 2020). There is increasing interest in *S. latissima*

72   farming along the European coasts ranging from Norway to Portugal where an

73   increasing number of commercial farms are set up in coastal systems (Peteiro and

74   Freire, 2013; Azevedo et al., 2016). It is common practice to set up trial farms and

75   conduct systematic planning before establishing large-scale culture activities in a

76   coastal system (Buck and Buchholz, 2005; Nielsen et al., 2014; Broch et al., 2019).

77   Given the interactions between the seaweeds and environmental factors (light,

78   temperature, nutrients, currents, salinity, etc.), the farm site and deployment and

79   harvest time are crucial to the production, chemical composition, and the

80   bioremediation effects of *S. latissima* (Marinho et al., 2015; Boderskov et al., 2016;

81   Bruhn et al., 2016; Nielsen et al., 2016; Sharma et al., 2019; de Jong et al., 2021). It is

82   also important to understand the carrying capacity of an ecosystem in regards to

83   seaweed cultivation when planning the culture plot, which has not been as extensively

84   discussed as other (e.g., fish, shellfish, shrimp etc.) forms of aquaculture (Shi et al.,

85   2011; Filgueira et al., 2015).

86   Carrying capacity (CC) is the "maximum" stock size that an ecosystem can

87   support and has multiple dimensions (Smaal and van Duren, 2019). The maximum

88   farm density and/or farmed area cannot exceed the level that a system can

89   accommodate in terms of space, water depth, and other physical conditions (physical

90   CC), that brings unacceptable ecological (ecological CC) or social disturbances

91   (social CC), or that depletes the resources and reduces the seafood quality or overall

92   yield (production CC). While the physical CC can be evaluated with fieldwork, GIS-

93   based methods, and numerical models, the other three CC concepts are somewhat

94   subjective depending on how ecosystem managers understand the "unacceptable

95   disturbance" or balance the aquaculture density with the seafood quality. In shellfish

96   culture, numerical models are applied to calculate the filtration capacity, primary

97   productivity, and water renewal efficiency and provide a quantitative assessment of

98   the CCs (e.g., Guyondet et al., 2015; Jiang et al., 2019a), which should be applicable

99   in seaweed cultivation as well where nutrient assimilation capacity is the equivalent of

100   filtration capacity.

101   A number of numerical seaweed models have been developed for various

102   purposes in prior studies, from statistical to mechanistic models with different

103   complexity (Petrell et al., 1993; Duarte and Ferreira, 1997; de Guimaraens et al.,

104   2005; Ren et al., 2014; Zhang et al., 2016; Lavaud et al., 2020). A mechanistic model

105   is usually formulated to address physiological processes including photosynthesis,

106   nutrient uptake and storage, biomass accumulation, respiration, etc. (Broch and

107   Slagstad, 2012). A seaweed model coupled with a hydrodynamic-biogeochemical

108   model may account for the environmental influences on seaweed growth dynamics

109   (Aveytua-Alcázar et al., 2008; Shi et al., 2011; Broch et al., 2019) and are practical

110   tools for CC assessment in ecosystems planned for seaweed farming.

111   We conducted a modeling study to evaluate the production and ecological CCs in

112   the Eastern Scheldt, a Dutch coastal bay where small-scale farming of *S. latissima* has

113   recently been piloted (van Oirschot et al., 2017). To this end, a *S. latissima* growth

114   module adapted from Broch and Slagstad (2012) was implemented into a recently

115   developed hydrodynamic-biogeochemical model (Jiang et al., 2020). The simulated *S.*

116   *latissima* growth and chemical composition were compared against data measured in

117   the seaweed farms and experimental tanks and assessed in response to various

118   hypothetical farming extents. The modeling approach is designed to provide

119   quantitative CC estimation for ecosystem managers and can be transferred to other

120   regions where seaweed farming is emerging.

121   **Methods**

122   ***The study area***

123   The Eastern Scheldt is a 350-km^2 coastal bay in the Southwest Delta region of the

124   Netherlands and is connected to the North Sea through a storm surge barrier (Figure

125   1). The shallow (avg. ~7 m) basin is featured by several tidal channels with a

126   maximum depth of ~50 m and flanking shoals, 110 km^2 of which are tidal flats. Due

127   to the Delta Works established in the 1980s, freshwater discharge into the Eastern

128   Scheldt is limited (Ysebaert et al., 2016) and semi-diurnal tides, with the mean range

129   of 2.5–3.4 m, exert a dominant influence on the water renewal of the bay (Jiang et al.,

130   2019b). The basin is mostly well-mixed with a salinity of 30–33 (Wetsteyn and

131   Kromkamp, 1994).

132   The Eastern Scheldt is known for its shellfish farming industry, including the

133   cultured species blue mussels (*Mytilus edulis*) and Pacific oysters (*Magallana gigas*).

134   The wild cockles (*Cerastoderma edule*) are also dominant benthic filter feeders

135   (Smaal et al 2013; Jiang et al., 2019b). Primary production, fueled by allochthonous

136   (transported from the adjacent North Sea) and autochthonous (regenerated internally)

137   nutrients, supports the large bivalve stock in the bay, but both primary production and

138   bivalve stocks decreased from the 1980s to 2010s (Smaal et al., 2013). Farming of *S.*

139   *latissima* has been piloted in the Eastern Scheldt for potential industrial scale-up since

140   2011 (van der Linden, 2014). In order to prevent the expanding seaweed farms from

141   interfering unacceptably with the existing phytoplankton and shellfish populations

142   and optimize the planning process, the CCs of the Eastern Scheldt for *S. latissima*

143   cultivation need to be assessed.

144   ***Field data***

145   The *S. latissima* seedlings were deployed and subsequently monitored at three sites in

146   the Eastern Scheldt: (1) Jacoba Harbor, (2) Neeltje Jans, and (3) NIOZ (Royal

147   Netherlands Institute for Sea Research), Yerseke. These pilot sites will be named as

148   numbers hereafter. Suspended ropes were used for seaweed at Sites 1 and 2, while

149   Site 3 included free-floating individuals that were cultivated in seaweed tanks with

150   continuously flushed water from the Eastern Scheldt. Information about the NIOZ

151   seaweed tanks is provided on the webpage

152   (https://www.nioz.nl/en/research/expertise/seaweed-centre). *S. latissima* individuals

153   were sampled on a biweekly to monthly basis (sometimes interrupted by the COVID-

154   19 pandemic) for monitoring frond area (cm^{-2}, all three sites) and dry weight (g, Sites

155   1 and 2) (Table 1). The frond area was determined using photographs, which were

156   analyzed in ImageJ (https://imagej.nih.gov/ij/). Dry weight was determined after

157   drying kelp tissues at 70 °C until stable weights were established. The culture density

158   at Site 1 was about 71 ind (individuals) m^{-2}, which was estimated prior to harvest by

159   the overall dry weight per meter line at harvest divided by the mean dry weight per

160   individual and the interval distance between two parallel lines (1.3 m). Note that only

161   the individual and total blades were weighed when estimating the farming density.

162   The farming density at Site 2 was unfortunately not recorded. At Site 3, each set of 5

163   individuals was grown in one 1400 L seaweed tank, so the density is much lower than

164   at Sites 1 and 2. The water temperature at Sites 1 and 2 were continuously measured

165   by HOBO temperature loggers, and the surrounding water was sampled to quantify

166   DIN (dissolved inorganic nitrogen) concentrations using a SEAL QuAAtro segmented

167   flow analyzer. Tissue samples were collected from Site 1, in which bulk carbon and

168   nitrogen contents (%C and N%) were determined. The sample size and measured

169   indices are listed in Table 1.

170   ***The hydrodynamic-biogeochemical-kelp model***

171   Physical conditions of the Eastern Scheldt and part of the adjacent North Sea is

172   simulated by the open-source hydrodynamic model GETM (General Estuarine

173   Transport Model, https://getm.eu/) on a 300 m × 300 m Cartesian grid with 10 sigma

174   layers. The biogeochemical processes were simulated by a NPZD (nutrient-

175   phytoplankton-zooplankton-detritus) framework in FABM (the Framework for

176   Aquatic Biogeochemical Models, available at https://github.com/fabm-model/fabm).

177   The nitrogen-based NPZD model includes the benthic filtration capacity estimated by

178   the observed shellfish biomass and filtration rate (annual survey data collected by

179   Wageningen Marine Research, https://shiny.wur.nl/Schelpdiermonitor_Delta). The

180   simulation was driven by realistic atmospheric forcing and boundary conditions, and

181   we refer to earlier papers (Jiang et al., 2019a, 2020) for detailed description of model

182   settings except for those related to the kelp module. The coupled model was calibrated

183   and validated using the two-year (2009–2010) observational data at four tide gauges

184   (used for water elevation records), five ADCP (used for current measurements)

185   stations, seven CTD (used for temperature and salinity measurements) stations, 11

186   nutrient and chlorophyll a stations in the Eastern Scheldt (Jiang et al., 2019a, 2020).

187   The simulation-observation correlation coefficients are above 0.9 for hydrodynamic

188   variables (Jiang et al., 2019a) and over 0.8 for chlorophyll a and DIN (Jiang et al.,

189   2020).

190   A *S. latissima* module that was modified based on the kelp model by Broch and

191   Slagstad (2012) was added to the NPZD framework as another primary producer,

192   competing light and inorganic nutrients with phytoplankton (Figure 2). The model is a

193   polyculture setup with both cultured bivalves and seaweed considered in the

194   ecosystem. Bivalves feed on phytoplankton, zooplankton, and detritus and release

195   inorganic nutrients into the seawater by respiration and excretion (Figure 2). The

196   bivalve biomass and physiological rates are described by Jiang et al. (2019a, 2020). In

197   contrast to free-floating phytoplankton, *S. latissima* was fixed at surface down to three

198   meters to mimic the cultured individuals and not subject to physical transport. The *S.*

199 *latissima* simulation started in November, 2009 and ended in June, 2010 to

200 accommodate the cultivation cycle. The culture density at Site 1 (71 ind m^{-2}) was

201 adopted and kept constant assuming no harvest or grazing mortality during the eight-

202 month growth. Note that the wild seaweed is not considered in the model for lack of

203 the distribution and biomass data. Three state variables associated with the *S.*

204 *latissima* biomass (the structural carbon, reserve carbon, and reserve nitrogen) were

205 implemented in the unit of mmol ind^{-1}. Formulations, variables, and parameters are

206 explained in Tables 2 and 3, respectively, which mainly focus on the differences of

207 our model from the Broch and Slagstad (2012) model, including a change from mass

208 to molar units, addition of new processes (e.g., activity respiration, necrosis) and

209 parameters tuned for the Eastern Scheldt case. The state variables of the *S. latissima*

210 model were converted to the frond area, dry weight, %C and %N (Equations 10–13 in

211 Table 2) and compared with those measured in the three study sites during 2019–2020

212 to calibrate the model.

Model scenarios and CC assessment

214 Two types of scenarios were run in this study: the baseline scenario representing

215 the current pilot sites and idealized scenarios increasing the farming area

216 hypothetically. In the baseline scenario, five farm locations with existing or potential

217 pilot cultivation were set up in the model to cover the *S. latissima* pilot sites (Figure

218 3a). Owing to the grid size, each farm accounts for 0.09 km^2. In addition, an

219 increasing farming area was implemented in four model scenarios, covering about

220 1%, 3%, 10%, and 30% of the entire bay, respectively, where farm locations were

221 uniformly distributed not considering any potential (physical) conflict with other user

222 functions (Figure 3). Through these scenarios, effects of expanding *S. latissima*

223 farming on biomass production, nutrients, and phytoplankton were studied, based on

224 which the CCs of the *S. latissima* cultivation in the Eastern Scheldt can be assessed.

225 **Results**

226 ***Comparison of model results to observations***

227 The model output in the baseline scenario was compared with measurements in the *S.*

228 *latissima* study sites. The simulated temperature in 2009–2010 was two to three

229 degrees cooler than the observations at Sites 1 and 2 in spring 2020 (Figure 4a). Both

230 modeled and observed DIN concentrations were highest and highly variable in winter

231 and sharply decreased after the spring bloom (Figure 4b). The DIN depletion was

232 slightly overestimated in late spring (Figure 4b). Overall, the simulated water

233 temperature and nutrients captured the general seasonal pattern measured in the

234 Eastern Scheldt cultivation sites in 2020 and were used to drive the *S. latissima*

235 simulation.

236   The modeled *S. latissima* growth was comparable to the measurements at three

237 sampling sites (Figure 5). The simulated frond area, an indicator of structural carbon

238 (Table 2), grew fast before slowing down in May and June (Figure 5a). The *S.*

239 *latissima* individuals at Site 3 that were cultured with continuously flushed Eastern

240 Scheldt water showed a higher growth rate than those cultured on long lines at other

241 sites (Figure 5a). Our modeled *S. latissima* exhibited a similar final frond size to the

242 observations despite an underestimated frond area in February and March (Figure 5a).

243   Dry weight is the sum of reserve and structural mass in *S. latissima* and displayed a

244   better agreement between modeled and measured data (Figure 5b).

245   In addition to the frond area and dry weight, seasonal variations of the

246   modeled %C and %N were consistent with the measurements at Site 1 (Figure 6).

247   Both the modeled and measured %C was minimal in winter and gradually increased

248   in spring (Figure 6a). In contrast, %N showed a winter maximum and declined from

249   spring to summer (Figure 6b). As a result of the underestimation of DIN in late spring

250   (Figure 4b), the model underestimated the *S. latissima* %N (Figure 6b) and therefore

251   overestimated the C:N ratio in May and June (Figure 6c).

252   ***The impact of increasing* S. latissima *farming area in the Eastern Scheldt***

253   With the increasing area for *S. latissima* cultivation, the total DIN consumption was

254   enhanced, causing an earlier DIN depletion and lower concentration in late spring

255   (Figure 7a). Compared to the baseline scenario, the average DIN concentration in late

256   June decreased by 4.8%, 12.4%, 34.9%, and 73.9% in the scenarios where farming

257   comprised about 1%, 3%, 10%, and 30% of the entire bay, respectively (Figure 8a).

258   Due to the introduced competition with the increasing *S. latissima* coverage, the other

259   primary producer, phytoplankton, was constrained, and the spring bloom magnitude

260   and duration were significantly reduced (Figure 7b). Reduction in phytoplankton net

261   primary production (NPP) was similar to that of biomass as a consequence of

262   introduced seaweed culture (Figure 7c). The average phytoplankton biomass in the

263   four scenarios expanding the *S. latissima* farming area was 2.1%, 5.6%, 16.2%, and

264   31.7% lower than the baseline scenario in June (Figure 8b). Owing to decreasing

abundance in phytoplankton, i.e., the primary prey of bivalves, shellfish biomass was

greatly affected by scale-up of *S. latissima* farms (Figure 8c). For instance, the blue

mussel biomass at harvest decreased by 3.4%, 8.9%, 29.3%, and 65.5% in these

scenarios, respectively (Figure 8c), which was much more than the reduction in

phytoplankton biomass (Figure 8b).

   In the *S. latissima* farming area, phytoplankton contributed to a larger proportion

of primary production before *S. latissima* took over from April to June (Figures 7c

and 9c). As the farming area expanded, the *S. latissima* growth was mainly affected

during this period of *S. latissima* dominating primary production, i.e., from April to

June (Figure 9). When the farming area was increased to around 1%, 3%, 10%, and

30% of the bay (representing a biomass of 3.4, 9.4, 28 and 75 kt in June), the overall

reductions in *S. latissima* peak NPP were 1.1%, 3.3%, 8.5%, and 25% (Figure 9c),

and the plants were on average 1.3%, 3.9%, 10.3%, and 28.3% smaller in terms of the

frond area, and 1.2%, 3.7%, 9.9%, 27.2% lighter in terms of dry weight in comparison

to the baseline scenario, respectively (Figure 10). In spite of the diminished individual

harvest size, the overall yield increased with the upscaled farming coverage in these

hypothetical scenarios (Figure 10). In addition to a smaller individual size, the *S.*

latissima cultured at a higher coverage in the Eastern Scheldt seemed to accumulate

less nitrogen but more carbon per individual, but the inter-scenario difference was far

less than the seasonal variation of %C and %N (Figure 11).

Discussion

Performance of the hydrodynamic-biogeochemical-kelp model

Driven by the three-dimensional hydrodynamic-biogeochemical model of the Eastern Scheldt, which was well verified (Jiang et al., 2019a, 2020), the individual-based seaweed model reproduced the *S. latissima* seasonal growth and chemical contents measured at field sites, which was also comparable to other *in situ* measurements and modeling studies.

The harvest frond size in the model (642 ± 232 cm^2) was within the range observed and modeled in the Norwegian coastal seas (350–900 cm^2, Broch et al., 2019). Compared to the individual frond area, production per meter line is a more common indicator of macroalgae culture in previous field and modeling studies. The yield in our study (0.94 ± 0.33 kg dry mass m^{-1} line) was lower than that measured in a Spanish coastal bay (1.4–1.9 kg dry mass m^{-1} line, Peteiro and Freire, 2013), in the upper range of the estimated production in the British and Dutch coastal waters (0.06–1.0 kg dry mass m^{-1} line, van der Molen et al., 2018), and much higher than the yield in a Danish fjord (<0.1 kg dry mass m^{-1} line, Bruhn et al., 2016). The inter-system variations are a result of various environmental influences. For example, *S. latissima* individuals in the filtered and flushed tanks at Site 3 grow faster than those in the other farms and modeled. These data at least corroborate that our modeled *S. latissima* yield is comparable to that in prior studies and within a reasonable range.

Seasonal variations of *S. latissima* C% and N% were significant but distinct, as found in our and previous studies (e.g., Black, 1950; Marinho et al., 2015; Sharma et

14

307   al., 2018). The internal nitrogen and protein contents usually accumulate in winter due

308   to the luxury uptake of the abundant DIN in the water column, while the carbon and

309   carbohydrate build up in summer as a consequence of the high photosynthesis rate

310   (Gevaert et al., 2001). Our model simulated this seasonal pattern and resolved %C

311   (20% to 40%) similar to that in other cultured populations (e.g., Gevaert et al., 2001;

312   Nielsen et al., 2014; Fossberg et al., 2018). The maximum nitrogen uptake rates (11.7

313   μmol cm^{-2} day^{-1}) in still (velocity < 0.01 m/s) waters are similar to that measured

314   under lab conditions (Lubsch and Timmermans, 2019), and %N that is primarily

315   controlled by the DIN concentration in the water column (Chapman et al., 1978;

316   Boderskov et al., 2016) varies considerably in different systems. Bruhn et al. (2016)

317   suggest a threshold tissue %N (1.88%) for maximum growth of *S. latissima*. The

318   nitrogen levels found in our study, cultured *S. latissima* in a eutrophic Danish fjord

319   (2.5%–4.8%, Bruhn et al., 2016), and wild species in the Easter English Channel

320   (2.2%–3.4%, Gevaert et al., 2001) were mostly above this level. In contrast, the

321   cultured *S. latissima* nitrogen level consistently fell below the critical value in

322   nutrient-depleted summer months in other systems (e.g., Sjøtun, 1993 as in Figure 6b;

323   Nielsen et al., 2014; Marinho et al., 2015; Fossberg et al., 2018), even reaching as low

324   as 0.14%, reported in inner Danish waters in August (Nielsen et al., 2016). These

325   studies reveal that the *S. latissima* growth and chemical composition are highly

326   variable and dependent on multiple environmental factors.

327   Our *S. latissima* model coupled with the three-dimensional hydrodynamic-

328   biogeochemical model has the advantages of simulating the *in situ* environmental

329　parameters (e.g., temperature, current velocity, nutrients, light) and thus resolving the

330　spatiotemporal variability in *S. latissima* biomass and chemical contents. However,

331　our model was not without limitations. For instance, our model was nitrogen-based

332　without considering phosphorus, although phosphorus can be limiting for short

333　periods in late spring in the Eastern Scheldt (Jiang et al., 2020). Although *S. latissima*

334　was found to maintain high growth rates for longer periods under phosphorus

335　limitation (Lubsch and Timmermans, 2019), the lack of phosphorus in the model may

336　have contributed to overestimation of DIN consumption by phytoplankton in late

337　spring and hence, underestimation of *S. latissima* %N in May and June. Additionally,

338　the model did not account for wave dissipation or turbulence changes caused by the

339　cultivation structures and seaweed thalli, which may generate intra-farm variations in

340　the nutrient uptake and photosynthesis rates (Wheeler, 1980; Stephens and Hepburn,

341　2014; Zhu et al., 2021). The current model considered only an annual farming cycle

342　(November to June) without addressing the macroalgal reproduction or epiphytes

343　infesting *S. latissima* in summer. Further development of the *S. latissima* model will

344　rely on the experimental data on these environmental and physiological processes. As

345　the model was capable of characterizing the seasonal *S. latissima* growth dynamics in

346　the Eastern Scheldt, it can be further used for CC assessments.

347　***The production carrying capacity***

348　The production CC is the stock size that supports the largest yield or highest quality in

349　a system (Dame and Prins, 1998). Food availability is usually the main driver of

350　production CC in aquaculture. For example, the plankton and organic matter in the

water is assessed to estimate the production CC in shellfish culture (Guyondet et al., 2015). For primary producers such as *S. latissima*, light and nutrients are potential limiting factors defining the production CC. In our application in the Eastern Scheldt, *S. latissima* individuals were growing in the surface water with little light limitation, so that nutrients (DIN) exert a first-order control on the production, especially in late spring.

When extending the farming scale in the Eastern Scheldt, DIN noticeably reduced, as seen in some Asian coastal bays with extensive seaweed farm coverage (Xiao et al., 2017). Decreasing NPP and individual harvest size with DIN shows that at large farming intensity competition for nutrients affected the *S. latissima* growth. However, competition for DIN were hardly noticeable until mid-April, when the overall *S. latissima* biomass built up and DIN became limited (<10 mmol m^{-3}). Moreover, the individual *S. latissima* growth was not proportionally affected by the increased farming area. For example, comparing the scenarios in which 10% versus 30% of the bay were used for seaweed cultivation and the number of cultivated *S. latissima* tripled, the peak seaweed NPP reduced by 18.1% (from 3718 mg C m^{-2} day^{-1} to 3044 mg C m^{-2} day^{-1}), and the average individual biomass (in dry weight) declined only by 19% (from 9.2 g ind^{-1} to 7.4 g ind^{-1}). Accordingly, the overall yield kept increasing with the farming area. If farm managers and the market accept smaller *S. latissima* size and lower %N, the model scenarios suggest that the production CC was not exceeded even when expanding the seaweed farms to occupy 30% of the Eastern Scheldt.

373   This is not the case everywhere. For instance, in the Chinese Sanggou Bay, a

374 10% reduction in the present farming scale may increase the final production of

375 *Saccharina japonica*, an extensively cultivated kelp species in East Asia (Shi et al.,

376 2011). In Sanggou Bay, the DIN concentration (1–16 mmol m^{-3}, Zhang et al., 2016)

377 was much lower than that in the Eastern Scheldt, so that the cultured *S. japonica*

378 experienced a longer time of nitrogen limitation and a stronger intra-species

379 competition for DIN (Shi et al., 2011). As argued in previous section, the DIN

380 concentration in the water column induces variations in the *S. latissima* %N in diverse

381 ecosystems, which implies that the production CC may vary substantially among

382 these systems. Therefore, results from our and other studies cannot simply be

383 extrapolated to other areas; rather the production CC of seaweed culture should be

384 comprehensively assessed considering at least the light climate and nutrient budget on

385 a system-specific and species-specific basis.

386 ***The ecological carrying capacity***

387 In contrast to the production CC, the ecological CC evaluates how the aquaculture

388 activities impact the ecosystem, particularly the predators, prey, and competitors of

389 the cultivated organism (Smaal and van Duren, 2019). In the Eastern Scheldt, the wild

390 and cultured shellfish is supported mainly by phytoplankton and particulate organic

391 matters (Smaal et al., 2013). Introducing the cultured *S. latissima* and adding its

392 competition with phytoplankton exert a potential influence to zooplankton and

393 bivalves, as well as the ecosystem structure, which highlights the importance of

394 assessing the ecological CC before large-scale farming of *S. latissima*.

395   With changing composition of primary producers in aquatic or terrestrial

396   systems, the overall ecosystem primary productivity seems to stay the same, but

397   partition of each primary producer is reallocated (Niklas and Enquist, 2001; Miller et

398   al., 2011). In our case, the overall *S. latissima* production increased with the farming

399   extent, while the modeled phytoplankton biomass and NPP during the spring bloom

400   decreased with the introduced competition with *S. latissima*. In the low-light winter

401   months, neither phytoplankton nor *S. latissima* were sensitive to the extent of the *S.*

402   *latissima* farming area. This indicates that their competition in spring was most likely

403   for nutrients rather than light. In fact, the cultivated *S. latissima* was implemented in

404   the surface layers with favorable light conditions. This is different from the

405   phytoplankton-macroalgae competition in natural waters of Mohawk Reef, California

406   USA, where phytoplankton may delay the growth of understory macroalgae by light

407   absorption in the surface layer (Miller et al., 2011). Our results indicate that it is only

408   at low DIN concentrations (approximately <10 mmol m^{-3}) when the phytoplankton

409   and seaweed biomass were notably constrained by extending the *S. latissima* farming

410   area.

411   Phytoplankton and macroalgae take different strategies against nitrogen

412   limitation. At low DIN concentrations, nitrogen uptake by macroalgae may not be as

413   fast as phytoplankton, partly indicated in the model by a lower DIN uptake half-

414   saturation concentration for phytoplankton (1 mmol m^{-3}, Jiang et al., 2020) than for *S.*

415   *latissima* (4 mmol m^{-3} or higher, Broch and Slagstad, 2012; Forbord et al., 2021).

416   Hence, phytoplankton develop the peak NPP earlier than *S. latissima* in each model

417 scenario, and similar phenomena are found by Miller et al. (2011). However,

418 phytoplankton can continue growing at a reduced rate for only a few days under

419 nutrient-depleted conditions, whereas macroalgae can store a substantial amount of

420 nitrogen in nutrient-rich seasons, which allows them to maintain growth in 7–34 days

421 under nitrogen limitation and adds to their advantages in the phytoplankton-kelp

422 competition (Pedersen and Borum, 1996). In our study, the effect of nitrogen

423 limitation on *S. latissima* NPP is 10–15 days later than that on phytoplankton NPP,

424 due to the seaweed nitrogen storage.

425 In eutrophic systems or around fish farms, seaweed cultivation can sequester the

426 excessive nutrients, so that the luxury nutrient uptake may provide positive ecological

427 services (Petrell et al., 1993; Broch et al., 2013; Handå et al., 2013; Reid et al., 2013;

428 Xiao et al., 2017). Thus, seaweed and fish are frequently incorporated into integrated

429 multi-trophic aquaculture (IMTA) for higher efficiency, and less waste (Marinho et

430 al., 2015; Fossberg et al., 2018). In contrast to the IMTA applications, in a system

431 where extensive shellfish culture has strong grazing pressure on phytoplankton

432 growth (Smaal et al., 2013), our study suggests that polyculture of shellfish and

433 seaweed may, to some extent, suppress the phytoplankton spring bloom and curtail

434 shellfish production to a larger extent. The ecological CC for *S. latissima* farming in

435 the Eastern Scheldt is subject to frame of reference adopted by the ecosystem

436 managers. Based on the chosen criteria, the ecological CC can be estimated according

437 to the "what if" scenarios of expanding the *S. latissima* farms in our or similar studies.

438 For example, in our case if it is deemed essential that the present phytoplankton and

439   shellfish standing stocks cannot be reduced by more than 5.6% and 8.9%,

440   respectively, the farming area should probably not exceed 10 km^2, representing 9.4 kt

441   harvest dry weight (Figure 10b), which is about 3% surface area of the bay.

442   ***Perspectives***

443   Due to its high economical value and the provision of ecosystem services (e.g.,

444   eutrophication mitigation, carbon sequestration), *S. latissima* cultivation is receiving

445   increasing interest and is fast developing around the world, especially in Europe and

446   North America (Krause-Jensen et al., 2018; Venolia et al., 2020). However, our study

447   suggests that the cons of expanding *S. latissima* cultivation should not be neglected.

448   In the Eastern Scheldt, the initiation and expansion of *S. latissima* farms introduce

449   intra- and inter-species competition for nutrients among primary producers, lower the

450   production of the existing shellfish culture, and likely change the ecological balance.

451   The susceptibility or vulnerability to large-scale *S. latissima* farming largely depends

452   on the ecosystem properties (oligotrophic versus eutrophic, high versus low turbidity,

453   complex versus simple food web structure, etc.). Therefore, the CC assessment, using

454   models and relevant ground truthing, should be carefully performed in each system

455   planned for *S. latissima* cultivation. Despite the fact that the production and ecological

456   CCs of seaweed farming vary substantially among systems, our study provides a

457   transferrable approach for such assessments. In order to further aid decision-making,

458   the three-dimensional hydrodynamic-biogeochemical-kelp model can be linked to

459   bioeconomic or social models (Timmermann et al., 2014; Tsani and Koundouri, 2018)

460   to add ecological and sociological dimensions of the CC evaluation in the future.

Conclusion

In this study, we presented a *S. latissima* model coupled with an existing three-dimensional hydrodynamic-biogeochemical model in order to assess the CC of *S. latissima* cultivation in a Dutch tidal bay, the Eastern Scheldt. The *S. latissima* model, based on Broch and Slagstad (2012), displayed reasonable skills in capturing the *in situ* measurements of *S. latissima* seasonal growth dynamics, %C, and %N. The CC assessments were conducted based on the hypothetical scenarios of increasing the farming area in the bay. Model results suggest that the production CC was likely not exceeded even when 30% of the Eastern Scheldt was used for cultivating *S. latissima* at the current farming density. However, with the expansion of the farming area, the primary production, biomass and duration of the spring phytoplankton bloom, and wild and cultured shellfish biomass were reduced. During this time, the competition between the cultured *S. latissima* and phytoplankton was more for nutrients (DIN) than light in the Eastern Scheldt. Overall, our study puts an emphasis on the ecological CC for seaweed cultivation that is likely reached earlier than the production CC in the bay. It is also implied that the CCs of seaweed cultivation may vary substantially with system properties (e.g., trophic status, turbidity, and ecosystem structure) and seaweed species (e.g., different nutrient uptake and photosynthetic kinetics). Conducting numerical CC assessments may be as important as setting up pilot farms before introducing seaweed cultures to a new region, to set the right scope or ambition for commercial production. Our modeling approach is easy to transfer to other estuarine and coastal systems for such applications.

References

Aveytua-Alcázar, L., Camacho-Ibar, V. F., Souza, A. J., Allen, J. I., and Torres, R. 2008. Modelling *Zostera marina* and *Ulva* spp. in a coastal lagoon. Ecological Modelling, 218: 354–366.

Azevedo, I. C., Marinho, G. S., Silva, D. M., and Sousa-Pinto, I. 2016. Pilot scale land-based cultivation of *Saccharina latissima* Linnaeus at southern European climate conditions: Growth and nutrient uptake at high temperatures.

505   Aquaculture, 459: 166–172.

506   Bartsch, I., Wiencke, C., Bischof, K., Buchholz, C. M., Buck, B. H., Eggert, A.,

507   Feuerpfeil, P., Hanelt, D., Jacobsen, S., Karez, R., Karsten, U., Molis, M.,

508   Roleda, M. Y., Schubert, H., Schumann, R., Valentin, K., Weinberger, F., and

509   Wiese, J. 2008. The genus *Laminaria sensu lato*: recent insights and

510   developments. European Journal of Phycology, 43: 1–86.

511   Black, W. A. P. 1950. The seasonal variation in weight and chemical composition of

512   the common British Laminariaceae. Journal of the Marine Biological Association

513   of the United Kingdom, 29: 45–72.

514   Boderskov, T., Nielsen, M. M., Rasmussen, M. B., Balsby, T. J. S., Macleod, A.,

515   Holdt, S. L., Sloth, J. J., and Bruhn, A. 2021. Effects of seeding method, timing

516   and site selection on the production and quality of sugar kelp, *Saccharina*

517   *latissima*: A Danish case study. Algal Research, 53, 102160.

518   Boderskov, T., Schmedes, P. S., Bruhn, A., Rasmussen, M. B., Nielsen, M. M., and

519   Pedersen, M. F. 2016. The effect of light and nutrient availability on growth,

520   nitrogen, and pigment contents of *Saccharina latissima* (Phaeophyceae) grown in

521   outdoor tanks, under natural variation of sunlight and temperature, during

522   autumn and early winter in Denmark. Journal of Applied Phycology, 28: 1153–

523   1165.

524   Broch, O. J., Alver, M. O., Bekkby, T., Gundersen, H., Forbord, S., Handå, A.,

525   Skjermo, J., and Hancke, K. 2019. The kelp cultivation potential in coastal and

526   offshore regions of Norway. Frontiers in Marine Science, 5: 529.

527   Broch, O. J., Ellingsen, I. H., Forbord, S., Wang, X., Volent, Z., Alver, M. O., Handå,

528   A., Anderson, K., Slagstad, D., Reitan, K. I., Olsen, Y., and Skjermo, J. 2013.

529   Modelling the cultivation and bioremediation potential of the kelp *Saccharina*

530   *latissima* in close proximity to an exposed salmon farm in Norway. Aquaculture

531   Environment Interactions, 4: 187–206.

532   Broch, O. J., and Slagstad, D. 2012. Modelling seasonal growth and composition of

533   the kelp *Saccharina latissima*. Journal of Applied Phycology, 24: 759–776.

534   Bruhn, A., Tørring, D. B., Thomsen, M., Canal-Vergés, P., Nielsen, M. M.,

535   Rasmussen, M. B., Eybye, K. L., Larsen, M. M., Balsby, T. J. S., and Petersen, J.

536   K. 2016. Impact of environmental conditions on biomass yield, quality, and bio-

537   mitigation capacity of *Saccharina latissima*. Aquaculture Environment

538   Interactions, 8: 619–636.

539   Buck, B. H., and Buchholz, C. M. 2005. Response of offshore cultivated *Laminaria*

540   *saccharina* to hydrodynamic forcing in the North Sea. Aquaculture, 250: 674–

541   691.

542   Campbell, I., Macleod, A., Sahlmann, C., Neves, L., Funderud, J., Øverland, M.,

543   Hughes, A. D., and Stanley, M. 2019. The environmental risks associated with

544   the development of seaweed farming in Europe-prioritizing key knowledge gaps.

545   Frontiers in Marine Science, 6, 107.

546   Chapman, A. R. O., Markham, J. W., and Lüning, K. 1978. Effects of nitrate

547   concentration on the growth and physiology of *Laminaria saccharina*

548   (Phaeophyta) in culture. Journal of Phycology, 14: 195–198.

549   Dame, R. F., and Prins, T. C. 1998. Bivalve carrying capacity in coastal ecosystems.

550   Aquatic Ecology, 31: 409–421.

551   de Guimaraens, M. A., de Moraes Paiva, A., and Coutinho, R. 2005. Modeling *Ulva*

552   spp. dynamics in a tropical upwelling region. Ecological Modelling, 188: 448–

553   460.

554   de Jong, D. L., Timmermans, K. R., de Winter, J. M., and Derksen, G. C. 2021.

555   Effects of nutrient availability and light intensity on the sterol content of

556   *Saccharina latissima* (Laminariales, Phaeophyceae). Journal of Applied

557   Phycology, 33: 1101–1113.

558   Duarte, P., and Ferreira, J. G. 1997. A model for the simulation of macroalgal

559   population dynamics and productivity. Ecological Modelling, 98: 199–214.

560   Duarte, C. M., Wu, J., Xiao, X., Bruhn, A., and Krause-Jensen, D. 2017. Can seaweed

561   farming play a role in climate change mitigation and adaptation?. Frontiers in

562   Marine Science, 4: 100.

563   FAO. 2020. The State of World Fisheries and Aquaculture 2020. Sustainability in

564   action. Rome. https://doi.org/10.4060/ca9229en.

565   Filgueira, R., Comeau, L. A., Guyondet, T., McKindsey, C. W., Byron, C. J. 2015.

566   Modelling carrying capacity of bivalve aquaculture: a review of definitions and

567   methods. In: Meyers, R.A. (Ed.), Encyclopedia of Sustainability Science and

568   Technology. Springer New York, pp. 1–33.

569   Forbord, S., Etter, S. A., Broch, O. J., Dahlen, V. R., and Olsen, Y. 2021. Initial short-

570   term nitrate uptake in juvenile, cultivated *Saccharina latissima* (Phaeophyceae)

571   of variable nutritional state. Aquatic Botany, 168: 103306.

572 Forbord, S., Skjermo, J., Arff, J., Handå, A., Reitan, K. I., Bjerregaard, R., and

573   Lüning, K. 2012. Development of *Saccharina latissima* (Phaeophyceae) kelp

574   hatcheries with year-round production of zoospores and juvenile sporophytes on

575   culture ropes for kelp aquaculture. Journal of Applied Phycology, 24: 393–399.

576 Fossberg, J., Forbord, S., Broch, O. J., Malzahn, A. M., Jansen, H., Handå, A., Førde,

577   H., Bergvik, M., Fleddum, A. L., Skjermo, J., and Olsen, Y. 2018. The potential

578   for upscaling kelp (*Saccharina latissima*) cultivation in salmon-driven integrated

579   multi-trophic aquaculture (IMTA). Frontiers in Marine Science, 5: 418.

580 Froehlich, H. E., Afflerbach, J. C., Frazier, M., and Halpern, B. S. 2019. Blue growth

581   potential to mitigate climate change through seaweed offsetting. Current Biology,

582   29: 3087–3093.

583 Gevaert, F., Davoult, D., Creach, A., Kling, R., Janquin, M. A., Seuront, L., and

584   Lemoine, Y. 2001. Carbon and nitrogen content of *Laminaria saccharina* in the

585   eastern English Channel: biometrics and seasonal variations. Journal of the

586   Marine Biological Association of the United Kingdom, 81: 727–734.

587 Guyondet, T., Comeau, L. A., Bacher, C., Grant, J., Rosland, R., Sonier, R., and

588   Filgueira, R. 2015. Climate change influences carrying capacity in a coastal

589   embayment dedicated to shellfish aquaculture. Estuaries and Coasts, 38: 1593–

590   1618.

591 Hasselström, L., Visch, W., Gröndahl, F., Nylund, G. M., and Pavia, H. 2018. The

592   impact of seaweed cultivation on ecosystem services - a case study from the west

593   coast of Sweden. Marine Pollution Bulletin, 133: 53–64.

594   Handå, A., Forbord, S., Wang, X., Broch, O. J., Dahle, S. W., Størseth, T. R., Reitan,

595   K. I., Olsen, Y., and Skjermo, J. 2013. Seasonal-and depth-dependent growth of

596   cultivated kelp (*Saccharina latissima*) in close proximity to salmon (*Salmo*

597   *salar*) aquaculture in Norway. Aquaculture, 414: 191–201.

598   Jiang, L., Gerkema, T., Kromkamp, J. C., Van Der Wal, D., Carrasco De La Cruz, P.

599   M., and Soetaert, K. 2020. Drivers of the spatial phytoplankton gradient in

600   estuarine–coastal systems: generic implications of a case study in a Dutch tidal

601   bay. Biogeosciences, 17: 4135–4152.

602   Jiang, L., Gerkema, T., Wijsman, J. W., and Soetaert, K. 2019a. Comparing physical

603   and biological impacts on seston renewal in a tidal bay with extensive shellfish

604   culture. Journal of Marine Systems, 194: 102–110.

605   Jiang, L., Soetaert, K., and Gerkema, T. 2019b. Decomposing the intra-annual

606   variability of flushing characteristics in a tidal bay along the North Sea. Journal

607   of Sea Research, 155: 101821.

608   Krause-Jensen, D., Lavery, P., Serrano, O., Marbà, N., Masque, P., and Duarte, C. M.

609   2018. Sequestration of macroalgal carbon: the elephant in the Blue Carbon room.

610   Biology Letters, 14: 20180236.

611   Lavaud, R., Filgueira, R., Nadeau, A., Steeves, L., and Guyondet, T. 2020. A Dynamic

612   Energy Budget model for the macroalga *Ulva lactuca*. Ecological Modelling,

613   418, 108922.

614   Lubsch, A., and Timmermans, K. R. 2019. Uptake kinetics and storage capacity of

615   dissolved inorganic phosphorus and corresponding dissolved inorganic nitrate

616   uptake in *Saccharina latissima* and *Laminaria digitata* (Phaeophyceae). Journal

617   of Phycology, 55: 637–650.

618 Marinho, G. S., Holdt, S. L., Birkeland, M. J., and Angelidaki, I. 2015. Commercial

619   cultivation and bioremediation potential of sugar kelp, *Saccharina latissima*, in

620   Danish waters. Journal of Applied Phycology, 27: 1963–1973.

621 Miller, R. J., Reed, D. C., and Brzezinski, M. A. 2011. Partitioning of primary

622   production among giant kelp (*Macrocystis pyrifera*), understory macroalgae, and

623   phytoplankton on a temperate reef. Limnology and Oceanography, 56: 119–132.

624 Nielsen, M. M., Krause-Jensen, D., Olesen, B., Thinggaard, R., Christensen, P. B.,

625   and Bruhn, A. 2014. Growth dynamics of *Saccharina latissima* (Laminariales,

626   Phaeophyceae) in Aarhus Bay, Denmark, and along the species' distribution

627   range. Marine Biology, 161: 2011–2022.

628 Nielsen, M. M., Manns, D., D'Este, M., Krause-Jensen, D., Rasmussen, M. B.,

629   Larsen, M. M., Alvarado-Morales, M., Angelidaki, I., and Bruhn, A. 2016.

630   Variation in biochemical composition of *Saccharina latissima* and *Laminaria*

631   *digitata* along an estuarine salinity gradient in inner Danish waters. Algal

632   Research, 13: 235–245.

633 Niklas, K. J., and Enquist, B. J. 2001. Invariant scaling relationships for interspecific

634   plant biomass production rates and body size. Proceedings of the National

635   Academy of Sciences, 98: 2922–2927.

636 Ogawa, H., and Fujita, M. 1997. The effect of fertilizer application on farming of the

637   seaweed *Undaria pinnatifida* (Laminariales, Phaeophyta). Phycological

638   Research, 45: 113–116.

639 Pedersen, M. F., and Borum, J. 1996. Nutrient control of algal growth in estuarine

640   waters. Nutrient limitation and the importance of nitrogen requirements and

641   nitrogen storage among phytoplankton and species of macroalgae. Marine

642   Ecology Progress Series, 142: 261–272.

643 Petrell, R. J., Tabrizi, K. M., Harrison, P. J., and Druehl, L. D. 1993. Mathematical

644   model of *Laminaria* production near a British Columbian salmon sea cage farm.

645   Journal of Applied Phycology, 5: 1–14.

646 Peteiro, C., and Freire, Ó. 2013. Biomass yield and morphological features of the

647   seaweed *Saccharina latissima* cultivated at two different sites in a coastal bay in

648   the Atlantic coast of Spain. Journal of Applied Phycology, 25: 205–213.

649 Reid, G. K., Chopin, T., Robinson, S. M. C., Azevedo, P., Quinton, M., and Belyea, E.

650   2013. Weight ratios of the kelps, *Alaria esculenta* and *Saccharina latissima*,

651   required to sequester dissolved inorganic nutrients and supply oxygen for

652   Atlantic salmon, *Salmo salar*, in integrated multi-trophic aquaculture systems.

653   Aquaculture, 408: 34–46.

654 Ren, J. S., Barr, N. G., Scheuer, K., Schiel, D. R., and Zeldis, J. 2014. A dynamic

655   growth model of macroalgae: application in an estuary recovering from treated

656   wastewater and earthquake-driven eutrophication. Estuarine, Coastal and Shelf

657   Science, 148: 59–69.

658 Sanderson, J. C., Dring, M. J., Davidson, K., and Kelly, M. S. 2012. Culture, yield

659   and bioremediation potential of *Palmaria palmata* (Linnaeus) Weber & Mohr

660   and *Saccharina latissima* (Linnaeus) CE Lane, C. Mayes, Druehl & GW

661   Saunders adjacent to fish farm cages in northwest Scotland. Aquaculture, 354:

662   128–135.

663   Sharma, S., Neves, L., Funderud, J., Mydland, L. T., Øverland, M., and Horn, S. J.

664   2018. Seasonal and depth variations in the chemical composition of cultivated

665   *Saccharina latissima*. Algal research, 32: 107–112.

666   Shi, J., Wei, H., Zhao, L., Yuan, Y., Fang, J., and Zhang, J. 2011. A physical-biological

667   coupled aquaculture model for a suspended aquaculture area of China.

668   Aquaculture, 318: 412–424.

669   Sjøtun, K. 1993. Seasonal lamina growth in two age groups of *Laminaria saccharina*

670   (L.) Lamour. in western Norway. Botanica Marina, 36: 433–441.

671   Smaal, A. C., Schellekens, T., van Stralen, M. R., and Kromkamp, J. C. 2013.

672   Decrease of the carrying capacity of the Oosterschelde estuary (SW Delta, NL)

673   for bivalve filter feeders due to overgrazing?. Aquaculture, 404: 28–34.

674   Smaal, A. C., and van Duren, L. A. 2019. Bivalve aquaculture carrying capacity:

675   concepts and assessment tools. In Goods and services of marine bivalves (pp.

676   451–483). Springer, Cham.

677   Stephens, T. A., and Hepburn, C. D. 2014. Mass-transfer gradients across kelp beds

678   influence *Macrocystis pyrifera* growth over small spatial scales. Marine Ecology

679   Progress Series, 515, 97–109.

680   Timmermann, K., Dinesen, G. E., Markager, S., Ravn-Jonsen, L., Bassompierre, M.,

681   Roth, E., and Støttrup, J. G. 2014. Development and use of a bioeconomic model

682   for management of mussel fisheries under different nutrient regimes in the

683   temperate estuary of the Limfjord, Denmark. Ecology and Society, 19: 14.

684   Tsani, S., and Koundouri, P. 2018. A methodological note for the development of

685   integrated aquaculture production models. Frontiers in Marine Science, 4: 406.

686   van der Linden, K. 2014. Dutch seaweed: An economic analysis of Dutch seaweed

687   (proteins) in the food and feed industry. MSc Thesis, Wageningen University.

688   van der Molen, J., Ruardij, P., Mooney, K., Kerrison, P., O'Connor, N. E., Gorman, E.,

689   Timmermans, K., Wright, S., Kelly, M., Hughes, A. D., and Capuzzo, E. 2018.

690   Modelling potential production of macroalgae farms in UK and Dutch coastal

691   waters. Biogeosciences, 15: 1123–1147.

692   van Oirschot, R., Thomas, J. B. E., Gröndahl, F., Fortuin, K. P., Brandenburg, W., and

693   Potting, J. 2017. Explorative environmental life cycle assessment for system

694   design of seaweed cultivation and drying. Algal Research, 27: 43–54.

695   Venolia, C. T., Lavaud, R., Green-Gavrielidis, L. A., Thornber, C., and Humphries, A.

696   T. 2020. Modeling the growth of sugar kelp (*Saccharina latissima*) in

697   aquaculture systems using Dynamic Energy Budget theory. Ecological

698   Modelling, 430: 109151.

699   Walls, A. M., Kennedy, R., Edwards, M. D., and Johnson, M. P. 2017. Impact of kelp

700   cultivation on the Ecological Status of benthic habitats and *Zostera marina*

701   seagrass biomass. Marine Pollution Bulletin, 123: 19–27.

702   Wetsteyn, L. P. M. J., and Kromkamp, J. C. 1994. Turbidity, nutrients and

703   phytoplankton primary production in the Oosterschelde (the Netherlands) before,

704   during and after a large-scale coastal engineering project (1980–1990).

705   Hydrobiologia, 282/283: 61–78.

706   Wheeler, W. N. (1980). Effect of boundary layer transport on the fixation of carbon by

707   the giant kelp *Macrocystis pyrifera*. Marine Biology, 56: 103–110.

708   Xiao, X., Agusti, S., Lin, F., Li, K., Pan, Y., Yu, Y., Zheng, Y., Wu, J., and Duarte, C.

709   M. 2017. Nutrient removal from Chinese coastal waters by large-scale seaweed

710   aquaculture. Scientific Reports, 7: 1–6.

711   Ysebaert, T., van der Hoek, D. J., Wortelboer, R., Wijsman, J. W., Tangelder, M., and

712   Nolte, A.: Management options for restoring estuarine dynamics and

713   implications for ecosystems: A quantitative approach for the Southwest Delta in

714   the Netherlands, Ocean Coastal Management, 121: 33–48.

715   Zhang, J., Wu, W., Ren, J. S., and Lin, F. 2016. A model for the growth of mariculture

716   kelp *Saccharina japonica* in Sanggou Bay, China. Aquaculture Environment

717   Interactions, 8: 273–283.

718   Zhu, Q., Zhu, Z., Nauta, R., Timmermans, K. R., Jiang, L., Cai, Y., Yang, Z., and

719   Gerkema, T. 2021. Impact of off-bottom seaweed cultivation on turbulent

720   variation in the hydrodynamic environment: A flume experiment study with

721   mimic and natural *Saccharina latissima* thalli. Science of the Total Environment,

722   797: 149048.

723

Table and Figures

Table 1 *S. latissima* sampling details in this study.

Sites	Measured indices	Sampling depth	Sampling time (No. of individuals)
1	Temperature, DIN, frond area, dry weight, %C, and %N	0.5–1 m	19-Feb-2020 (30), 2-Apr-2020 (30), 30-Apr-2020 (30), 9-Jun-2020 (30)
2	Temperature, DIN, frond area, dry weight	0.5–1 m	19-Mar-2020 (36), 15-Apr-2020 (46), 7-May-2020 (49), 26-May-2020 (48)
3	frond area	N.A.	20-Feb-2020 (5), 28-Feb-2020 (5), 5-Mar-2020 (6), 13-Mar-2020 (6)

726

727 **Table 2** Formulations used in the kelp model. Parameters and variables in each
728 equation are described in Table 3.

$$\frac{dSTRU\_C}{dt} = Gro - Ero - Nec \tag{1}$$

$$Gro = \mu_{max} \cdot f(A) \cdot f(DL) \cdot f_g(T) \cdot f(S) \cdot f(Q) \cdot STRU\_C \tag{2}$$

$$f(Q) = \min\left(1, \max\left(0, \left(1 - \max\left(\frac{qNS_{min}}{qNS}, \frac{qRS_{min}}{qRS}\right)\right)\right)\right) \tag{3}$$

$$Nec = r_b \cdot f_r(T) \cdot STRU\_C \cdot \left(1 - \frac{qRS^3}{qRS^3 + qRS_{min}^3}\right) \tag{4}$$

$$\frac{dRES\_C}{dt} = Pho \cdot (1 - eC) - Gro - Res - qRS \cdot Ero \tag{5}$$

$$Res = r_b \cdot f_r(T) \cdot \left(RES\_C + STRU\_C \cdot \frac{qRS^3}{qRS^3 + qRS_{min}^3}\right) + \gamma \cdot Gro \tag{6}$$

$$\frac{dRES\_N}{dt} = Nupt - NCstru \cdot Gro - qNS \cdot Ero \tag{7}$$

$$Nupt = r_{Nupt} \cdot f(DIN) \cdot f(U) \cdot f(q) \cdot STRU\_C \tag{8}$$

$$\frac{dDIN}{dt} = \frac{den}{Dep} \cdot (NCstru \cdot (Ero + Nec) + qNS \cdot Ero - Nupt) + Exc \tag{9}$$

$$A = qAS * STRU\_C \tag{10}$$

$$DW = 12 \text{ g (mol } C)^{-1} \cdot (STRU\_C + RES\_C) + 0.014 \text{ g (mol } N)^{-1}$$
$$\cdot (RES\_N + NCstru \cdot STRU\_C) \tag{11}$$

$$C\% = 12 \text{ g (mol } C)^{-1} \cdot (STRU\_C + RES\_C)/DW \tag{12}$$

$$N\% = 14 \text{ g (mol } N)^{-1} \cdot (RES\_N + NCstru \cdot STRU\_C)/DW \tag{13}$$

$$k = k_0 + k_s \cdot TSS + k_c \cdot (P + D) + k_{kelp} \tag{14}$$

729

Table 3 The main variables (bold) and parameters (underlined) in equations in Table 2. The variables and parameter that are the same as Broch and Slagstad (2012) and Broch et al. (2019) are asterisked.

STRU_C, structural carbon (mmol ind^{-1}); **t**, time (day); **Gro**, the kelp growth rate (mmol ind^{-1} day^{-1}); **Ero**, the kelp erosion rate (mmol ind^{-1} day^{-1})*; **Nec**, the kelp necrosis rate if the carbon reserve is depleted (mmol ind^{-1} day^{-1})	(1)
$\underline{\mu_{max}}$ = 0.18 day^{-1}, the maximum growth rate; **f(A)**, the effect of size on growth (dimensionless)*; **f(DL)**, the effect of daylength on growth (dimensionless)*; **f$_g$(T)**, the effect of temperature on growth (dimensionless)*; **f(S)**, the effect of salinity on growth (dimensionless)*; **f(Q)**, the effect of carbon or nitrogen limitation on growth (dimensionless)	(2)
qNS, the quota reserve nitrogen per structural carbon (mol N mol C^{-1}); $\underline{qNS_{min}}$ = 0.1, the minimum quota reserve nitrogen per structural carbon (mol N mol C^{-1}); **qRS**, the quota reserve carbon per structural carbon (mol C mol C^{-1}); $\underline{qRS_{min}}$ = 0.08, the minimum quota reserve nitrogen per structural carbon (mol N mol C^{-1})	(3)
$\underline{r_b}$ = 0.001 day^{-1}, the basal respiration rate; **f$_r$(T)**, the effect of temperature on respiration (dimensionless)*	(4)
RES_C, reserve carbon (mmol ind^{-1}); **Pho**, the photosynthesis rate (mmol ind^{-1} day^{-1})*; **eC**, carbon exudation fraction (dimensionless)*; **Res**, the respiration rate (mmol ind^{-1} day^{-1})	(5)
$\underline{\gamma}$ = 0.3, growth respiration, a fraction of growth	(6)
RES_N, reserve nitrogen (mmol ind^{-1}); **Nupt**, the kelp nitrogen uptake rate (mmol ind^{-1} day^{-1}); $\underline{NCstru}$ =0.1 mol N mol C^{-1}, structural nitrogen per structural carbon	(7)
$\underline{r_{Nupt}}$ = 0.5 mol N mol C^{-1} day^{-1}, the maximum nitrogen uptake rate per mole structural carbon; **f(DIN)**, the effect of water-column DIN concentration on its uptake (dimensionless)*; **f(U)**, the effect of current velocity on DIN uptake (dimensionless)*; **f(q)**, the effect of the nitrogen reserve on DIN uptake (dimensionless)*	(8)
$\underline{den}$ = 71 ind m^{-2}, the kelp farming density; **Dep**, the layer depth (m); **Exc**, the physical exchange and sources and sinks of DIN in the NPZD model (mmol m^{-3} day^{-1})	(9)
A, the kelp frond area (m^2 ind^{-1}); $\underline{qAS}$ = 0.0012 m^2 mmol C^{-1}, the kelp fond area per mole structural carbon	(10)
DW, the kelp dry weight (g ind^{-1})	(11)
C%, the kelp carbon content (dimensionless)	(12)
N%, the kelp nitrogen content (dimensionless)	(13)
k, the overall light attenuation coefficient, $\underline{k_0}$ = 0.038 m^{-1}, the background attenuation coefficient by water, $k_s \cdot$**TSS**, the attenuation coefficient by total suspended solids ($\underline{k_s}$ = 0.094 m^2 g^{-1}, **TSS** in g m^{-3}), $k_c \cdot$(**P** + **D**), the attenuation coefficient by phytoplankton and detritus ($\underline{k_c}$ = 0.008 m^2 mmol N^{-1}; **P** and **D**, phytoplankton biomass and detritus in mmol N m^{-3}), $\underline{k_{kelp}}$, the attenuation coefficient by kelp*	(14)
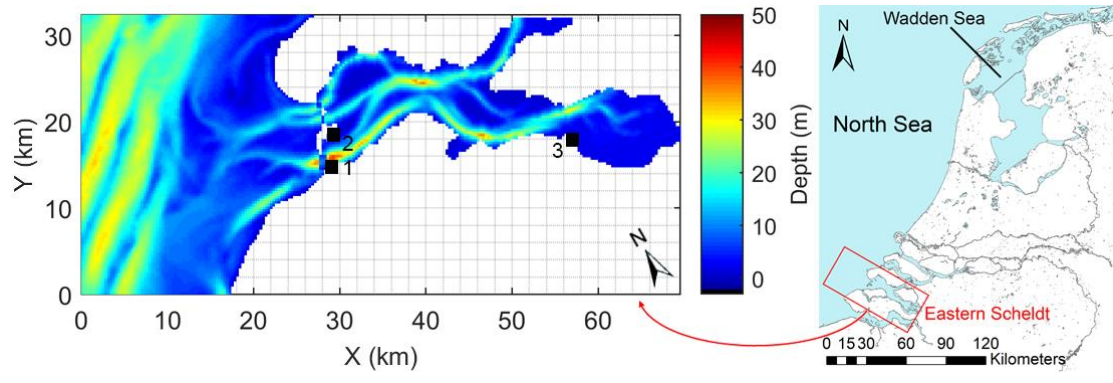
Figure 1. The location of the Eastern Scheldt (the right panel) and the model domain (the left panel). The three marked locations are the *S. latissima* sampling sites in this study. A storm surge barrier is located near Sites 1 and 2 (around X = 28 km).
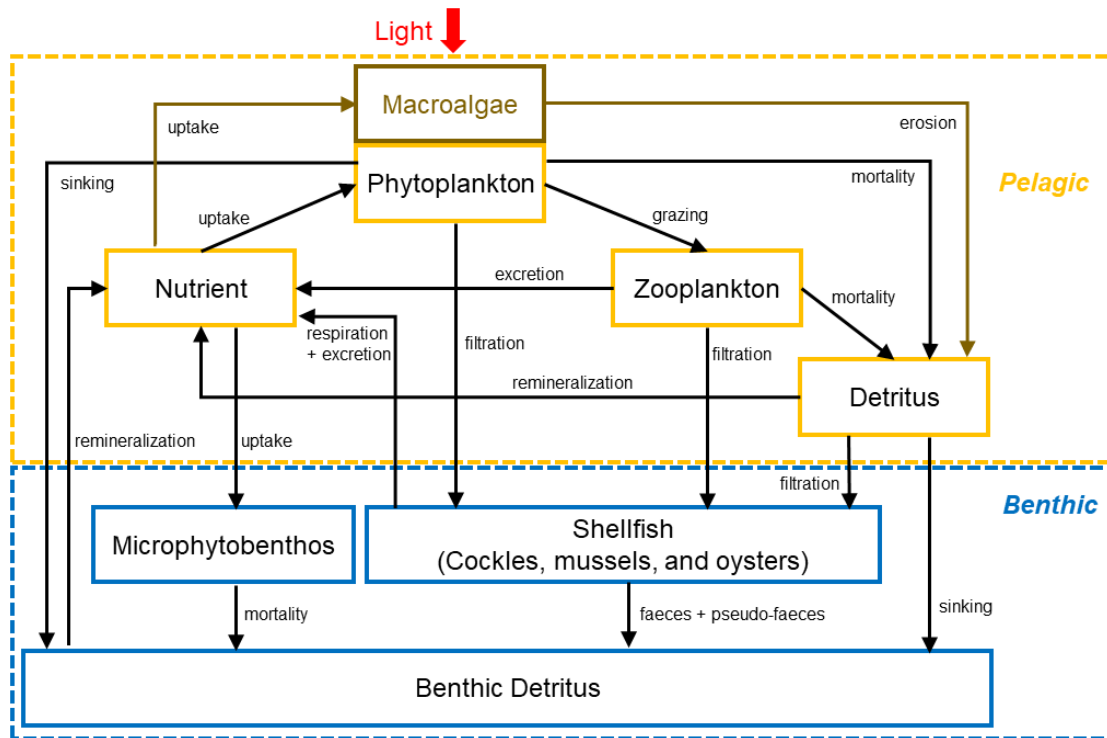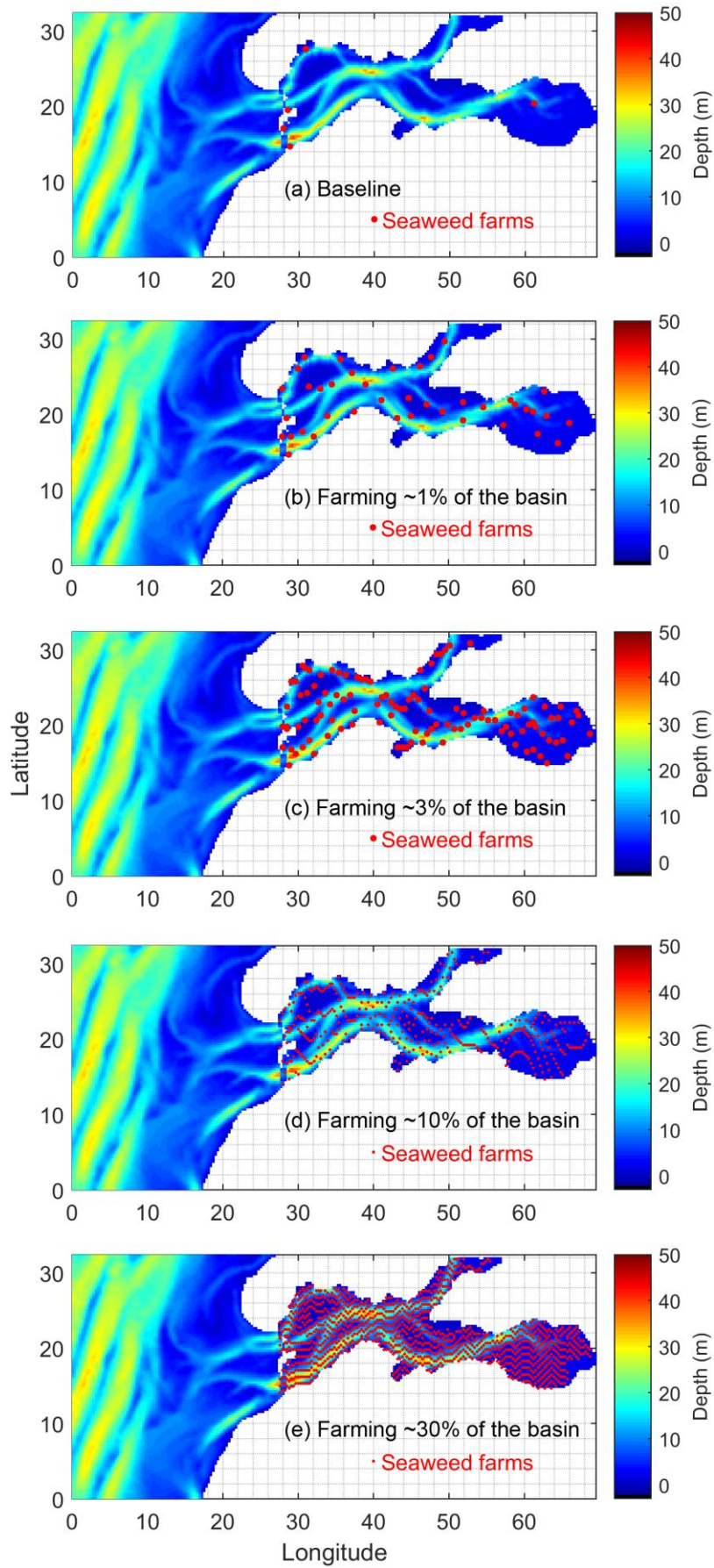
Figure 2. Conceptual diagram of the biogeochemical-kelp model. Boxes and arrows denote state variables and fluxes of nitrogen, respectively.
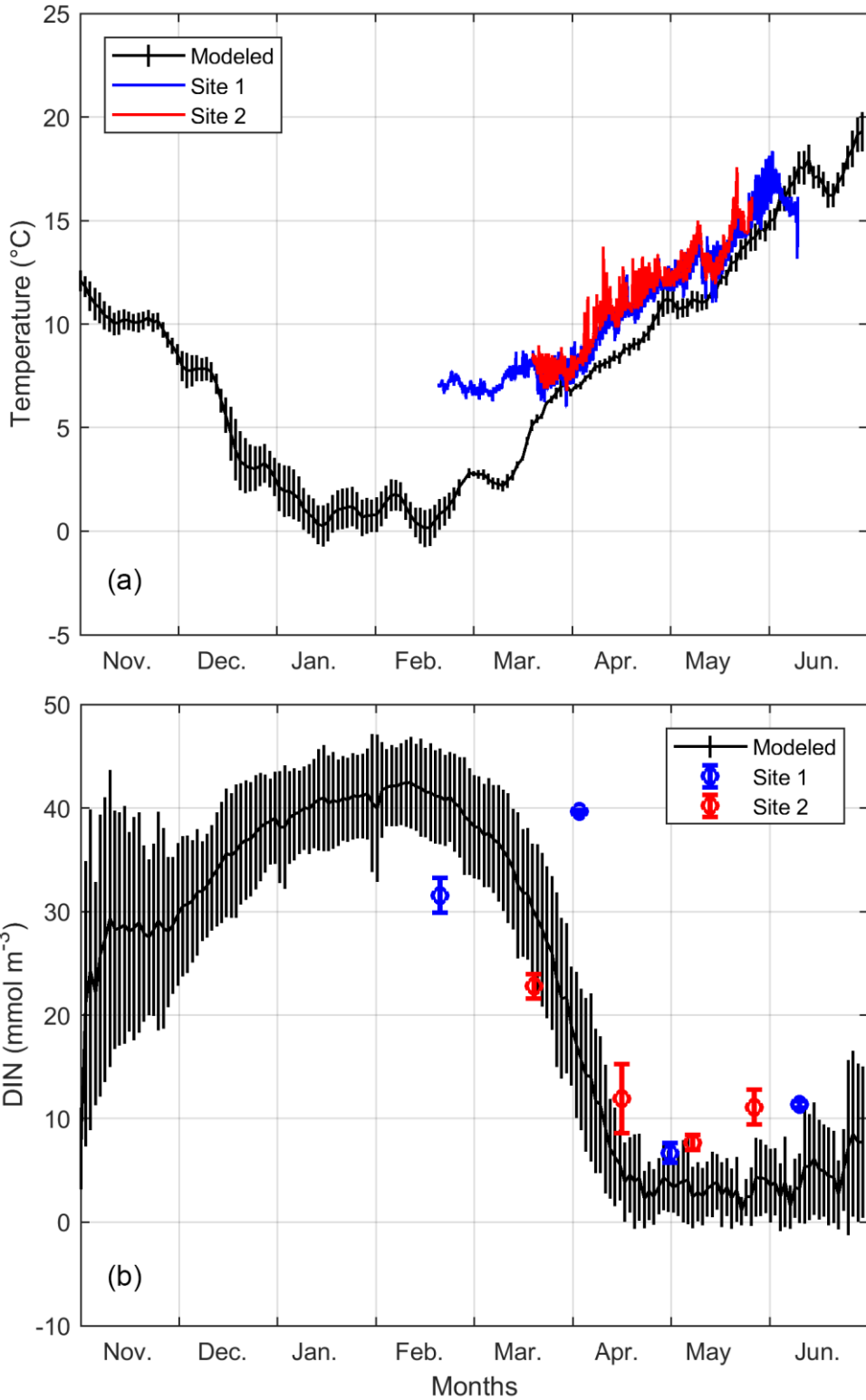
**Figure 3.** Farming locations in the numerical scenarios of this study.

**Figure 4.** Comparison of the modeled surface (a) temperature and (b) DIN concentration from November 2009 to June 2010 with observations at two sampling sites. See Figure 1 for sampling sites. The black lines show averages and standard deviations at the modeled farms in the baseline scenario (Figure 3a).

748
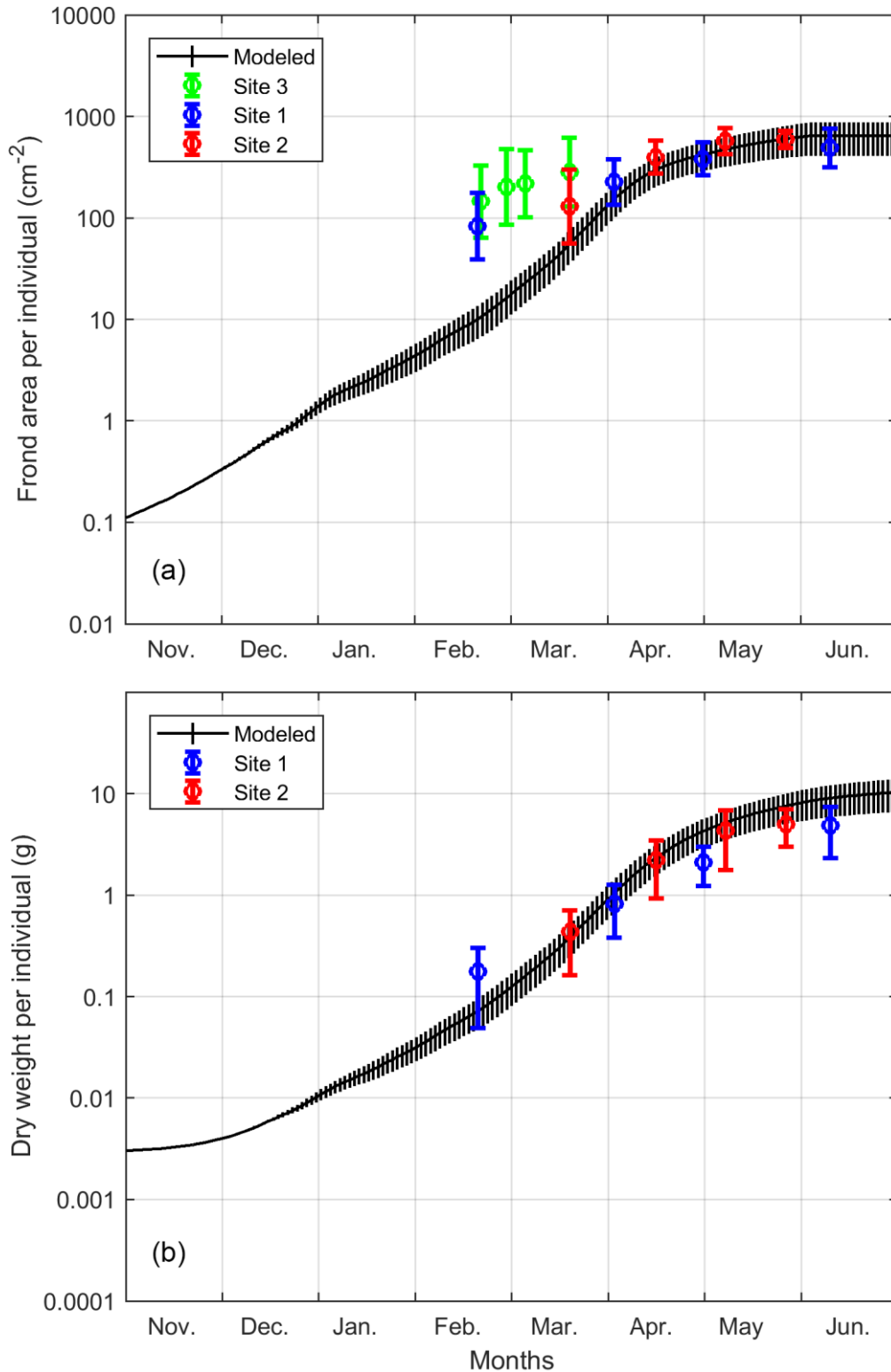
Figure 5. Comparison of the modeled *S. latissima* (a) frond area and (b) dry weight
from November 2009 to June 2010 with observations at three sampling sites. See
Figure 1 for sampling sites. The black lines show geometric averages and standard
deviations at the modeled farms in the baseline scenario (Figure 3a). Note that a
logarithmic scale is used for the y-axis.
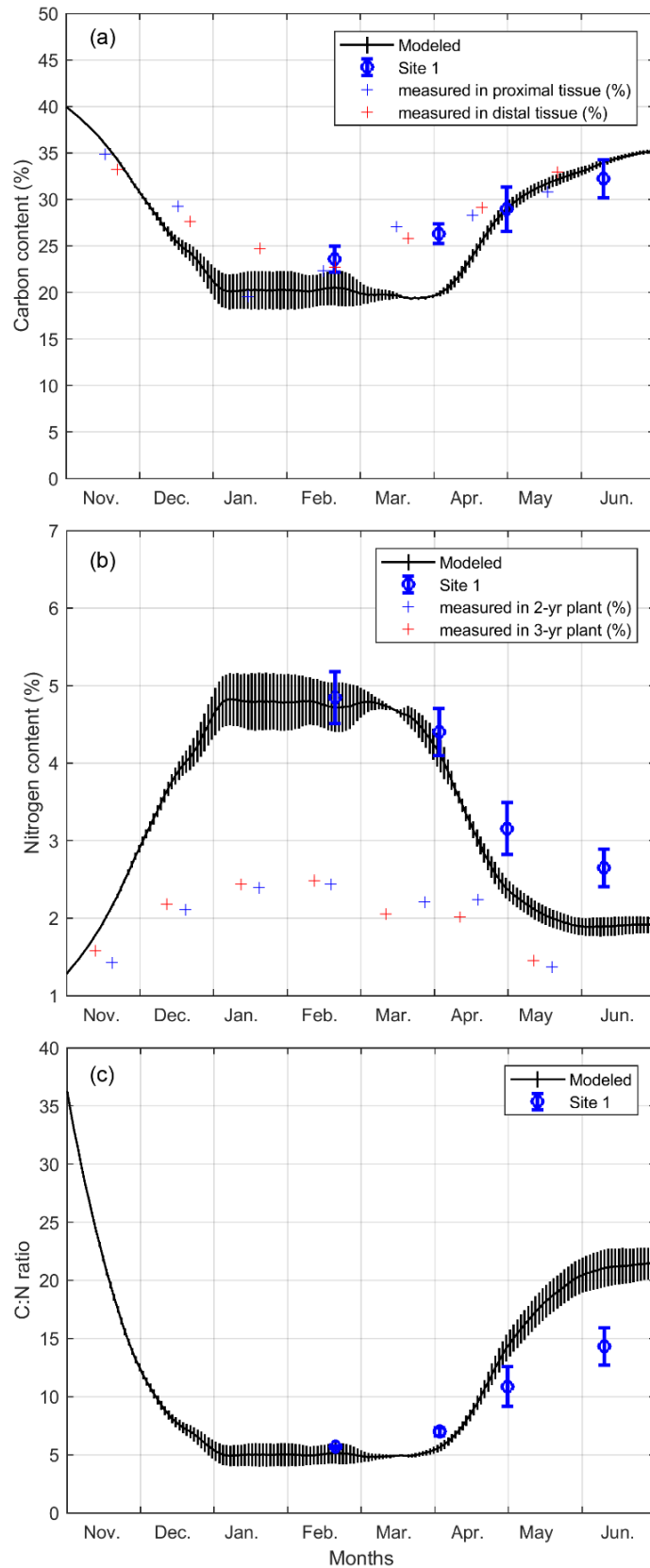
Figure 6. Comparison of the modeled *S. latissima* (a) %C, (b) %N, and (c) C:N ratio from November 2009 to June 2010 with observations at Site 1 and an earlier study (Sjøtun, 1993). See Figure 1 for sampling sites. The black lines show averages and standard deviations at the modeled farms in the baseline scenario (Figure 3a).
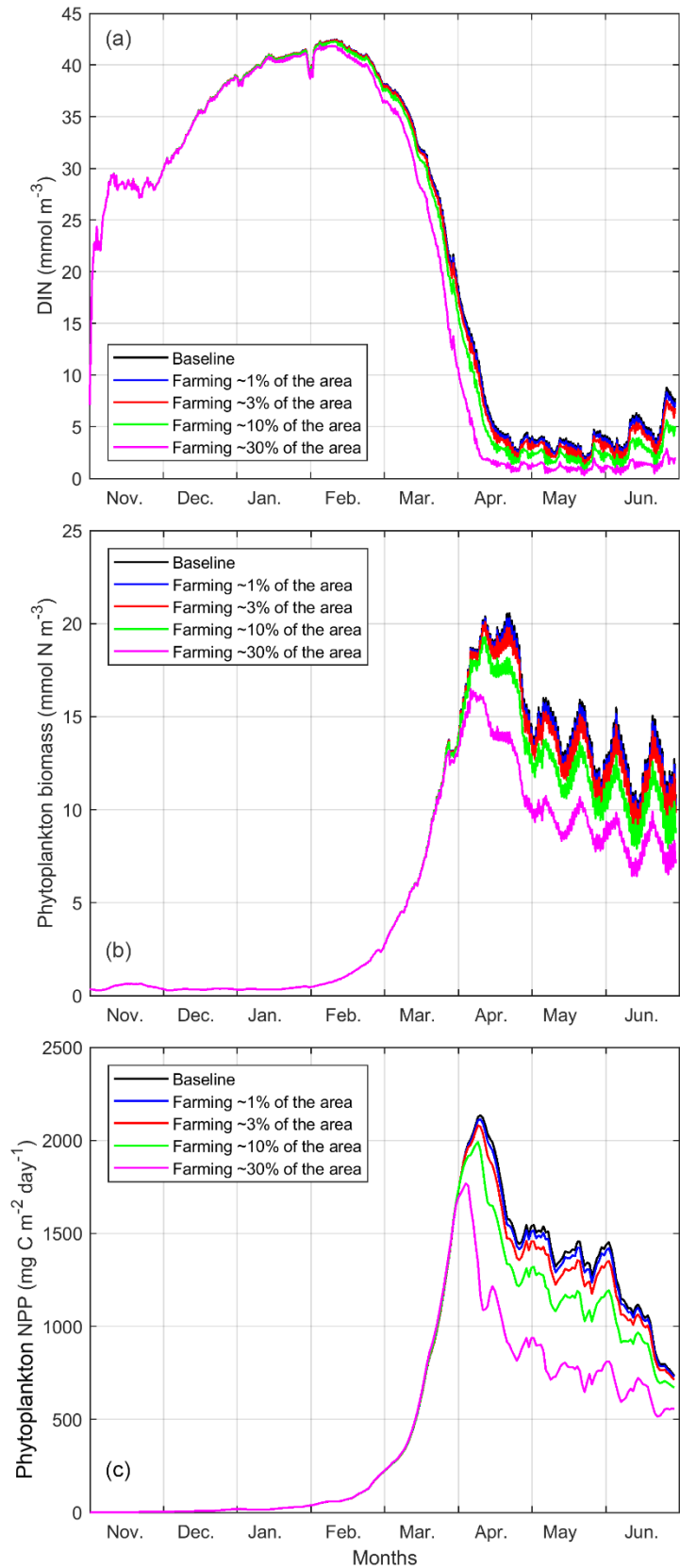
Figure 7. The modeled (a) DIN concentration, (b) phytoplankton biomass, and (c) phytoplankton net primary production (NPP) from November 2009 to June 2010 in scenarios varying farming areas (Figure 3). The presented data are averaged for five modeled farms shown in Figure 3a.
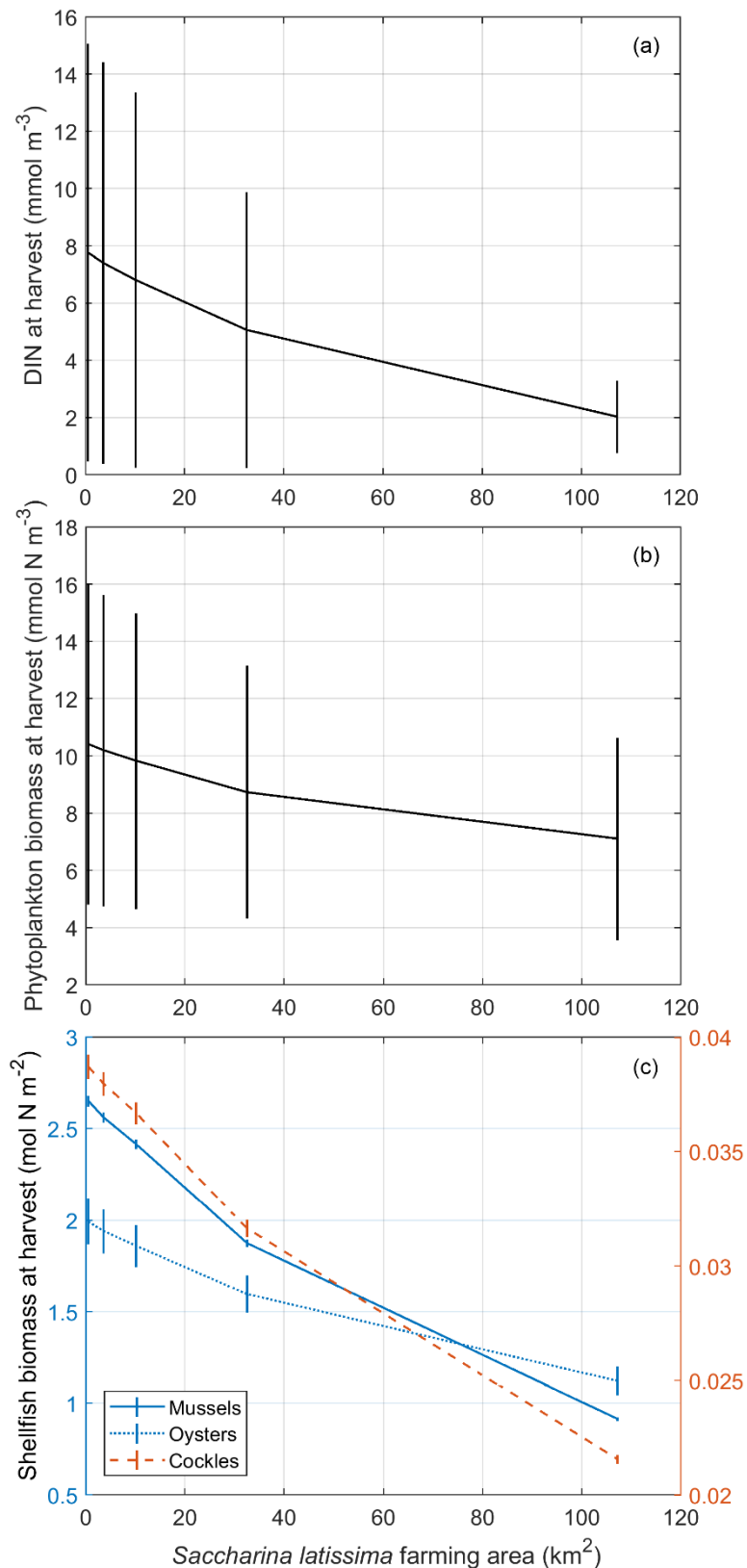
Figure 8. The modeled (a) DIN concentration, (b) phytoplankton biomass, and (c) shellfish biomass at *S. latissima* harvest time (30 June 2010) in scenarios varying seaweed farming areas (Figure 3). The presented data are averages and standard deviations for five modeled farms shown in Figure 3a. Standard deviations presented in panel (c) is 1% of the realistic value for better visualization.
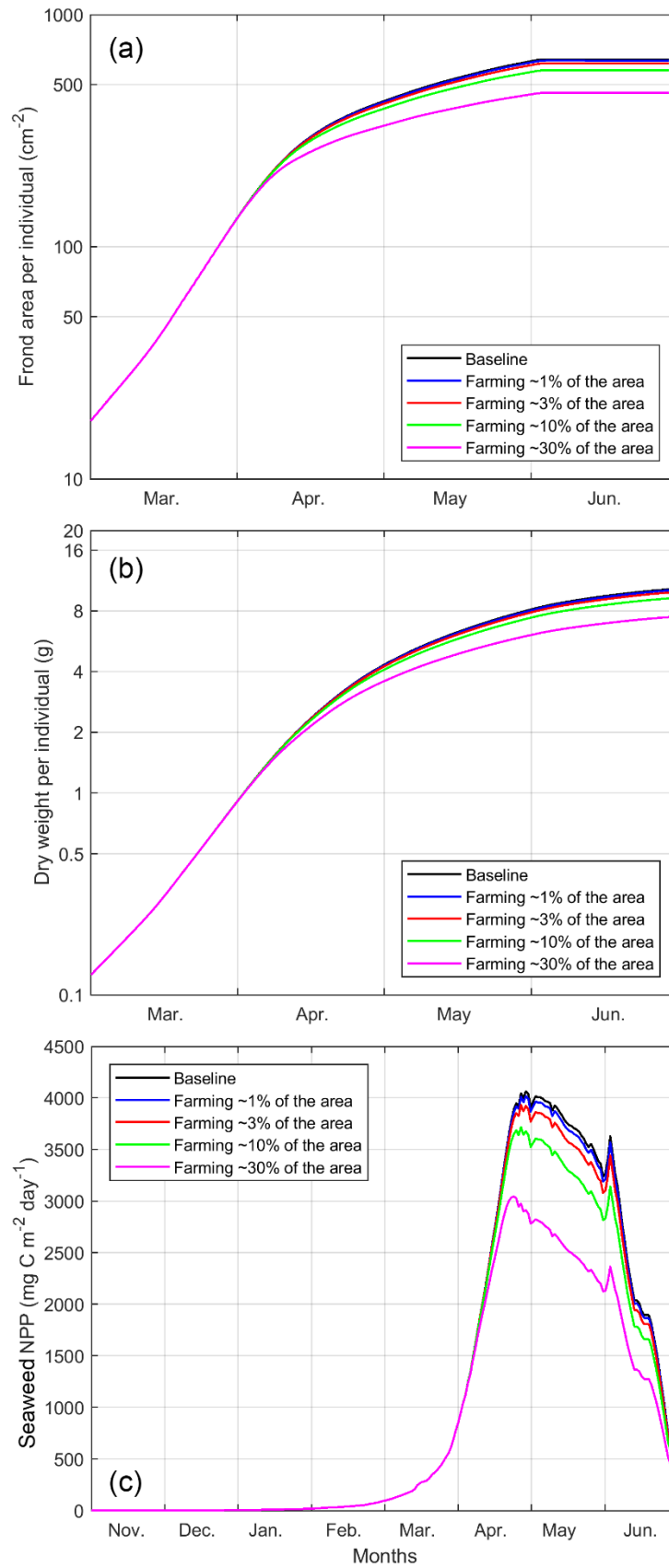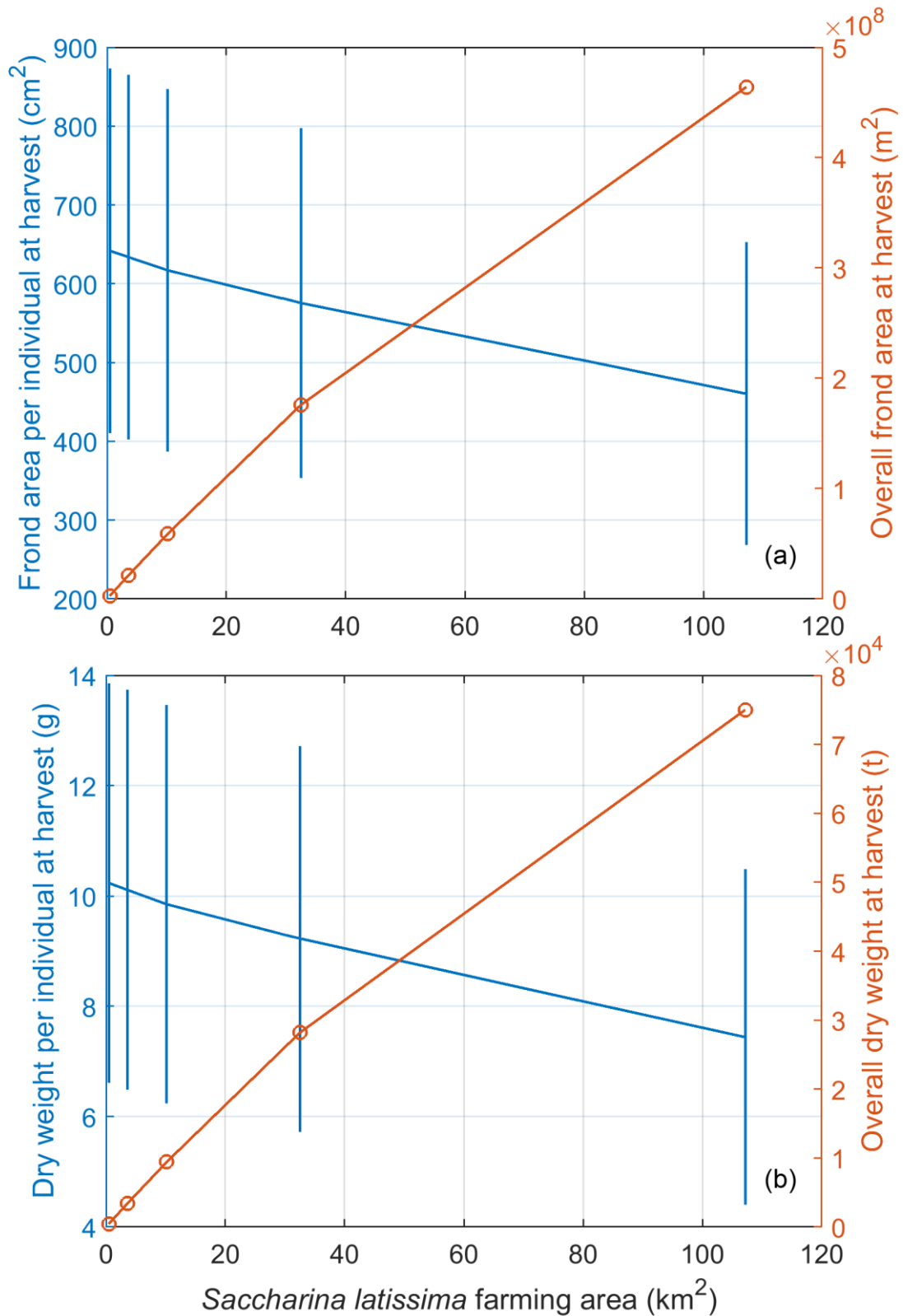
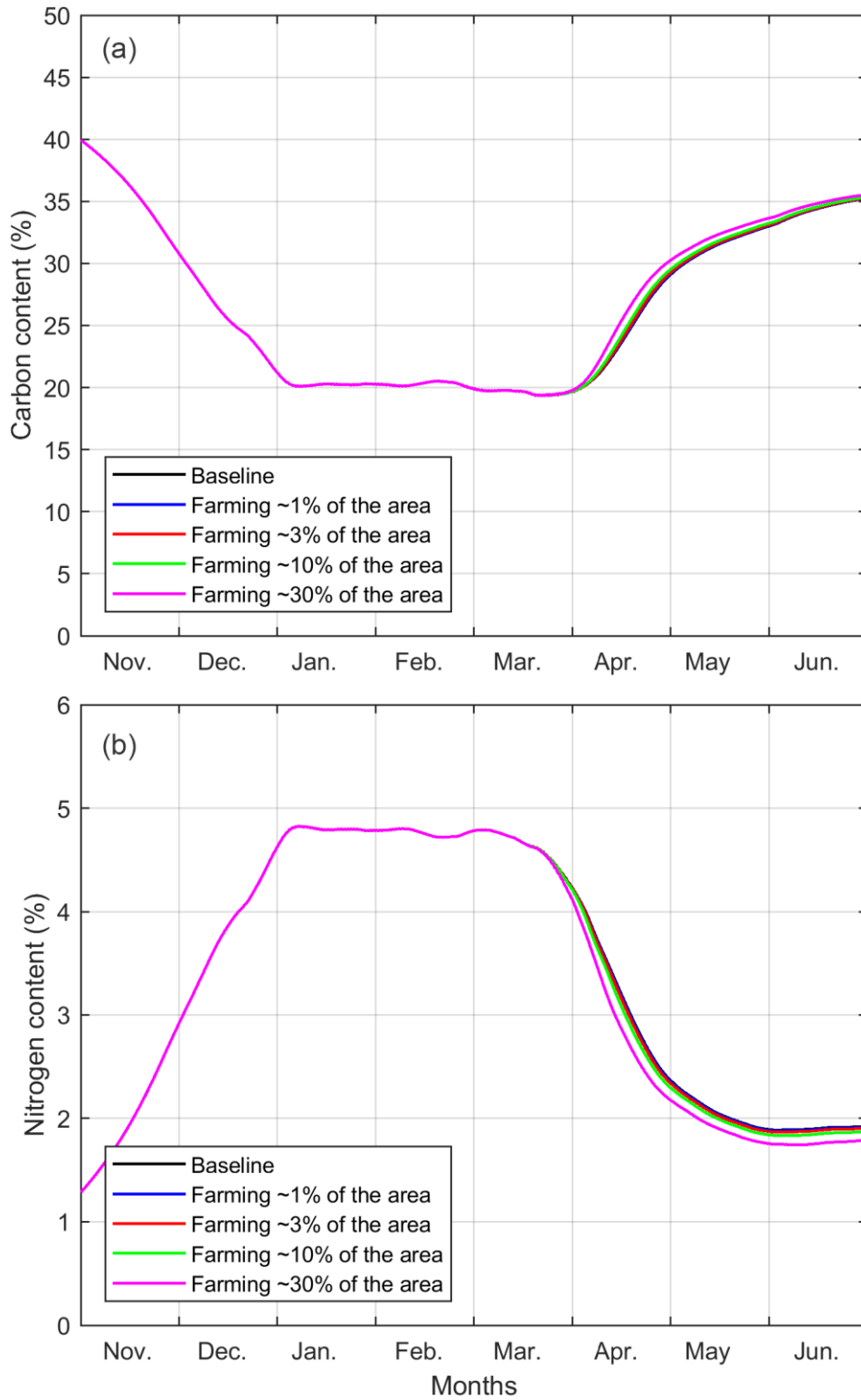**Figure 9.** The same as Figure 7, but for the *S. latissima* (a) frond area, (b) dry weight, and (c) net primary production (NPP). Note that a logarithmic scale is used for the y-axis and that the x-axis is zoomed in from March to June.

45

774

Figure 10. The modeled *S. latissima* (a) frond area and (b) dry weight at harvest time
(30 June 2010) in scenarios varying farming areas (Figure 3). The presented data are
averages and standard deviations for five modeled farms shown in Figure 3a.

46

Figure 11. The same as Figure 7, but for the *S. latissima* (a) %C and (b) %N.